RSC Advances

REVIEW

View Article Online
View Journal | View Issue

Cite this: *RSC Adv.*, 2022, **12**, 35744

Ti–Mn hydrogen storage alloys: from properties to applications

Jianjun Liu, Lei Sun, Jinggang Yang, Dongliang Guo, Dabing Chen, Liheng Yang and Peng Xiao *

Received 17th November 2022
Accepted 5th December 2022

DOI: 10.1039/d2ra07301c

rsc.li/rsc-advances

Efficient and safe storage of hydrogen is an important link in the process of hydrogen energy utilization. Hydrogen storage with hydrogen storage materials as the medium has the characteristics of high volumetric hydrogen storage density and good safety. Among many hydrogen storage materials, only rare earth-based and titanium-based hydrogen storage alloys have been applied thus far. In this work, current state-of-the-art research and applications of Ti–Mn hydrogen storage alloys are reviewed. Firstly, the hydrogen storage properties and regulation methods of binary to multicomponent Ti–Mn alloys are introduced. Then, the applications of Ti–Mn alloys in hydrogen storage, hydrogen compression and catalysis are discussed. Finally, the future research and development of Ti–Mn hydrogen storage alloys is proposed.

1 Introduction

Hydrogen is an ideal energy source with wide availability, abundant reserves, various utilization forms, high combustion calorific value and pollution-free combustion products. Hydrogen production by electrolysis of water can transform the surplus power from renewable energy (wind energy, solar energy, *etc.*) into hydrogen, which can realize the long-term storage of large-scale renewable energy. Hydrogen can be used to generate electricity and heat through fuel cells, be transported into the natural gas pipe network for residents to burn, be transported to hydrogen refueling stations to provide fuel for fuel cell vehicles, or be used as a raw material for synthetic ammonia, metal smelting and other industries.[1–5] The large-scale utilization of hydrogen energy involves many technical links, including electrolysis of water to produce hydrogen, storage and transport of hydrogen, fuel cells, hydrogen refueling infrastructure and other supporting technologies related to hydrogen utilization.[6] At normal conditions, the density of hydrogen is only 0.0899 kg m^{-3}, and it is flammable and explosive, with the explosion limit around 4–75.6% (volume fraction). In addition, high-pressure hydrogen can lead to hydrogen embrittlement of many metals. Therefore, the efficient, safe and high-density storage of hydrogen is one of the key bottleneck technologies for hydrogen energy utilization.[7]

Hydrogen can exist in the form of gas, liquid or solid, and correspondingly, hydrogen can be stored in the form of high-pressure gas, low-temperature liquid or solid hydride. High-pressure hydrogen storage is the most commonly used hydrogen storage method at present, which has the advantages of convenient hydrogen charging and discharging, but its volumetric hydrogen storage density is very low.[8] For example, a high-pressure hydrogen storage tank of 35 MPa only has a volumetric hydrogen storage density of about 20 kg H_2 m^{-3}. Generally, hydrogen storage density can be improved by increasing the storage pressure, but this will also increase the energy consumption of compression on the one hand, and put forward higher requirements on the pressure tolerance of hydrogen storage containers on the other hand, which leads to a sharp rise in costs.[9,10] For mobile application scenarios, high-pressure gaseous hydrogen storage is generally adopted, and carbon fiber reinforced composite lightweight hydrogen storage tank is used as the hydrogen storage container. At present, 70 MPa high pressure hydrogen storage tank has been commercialized. Cryogenic liquid hydrogen storage is a hydrogen storage method that stores the liquefied hydrogen in an adiabatic vessel, which has the advantage of high hydrogen storage density (higher than 50 kg H_2 m^{-3}). However, its liquefaction process consumes a lot of energy, requires high insulation performance of the container, and has the potential safety risk of hydrogen evaporation and leakage.[11,12] Low-temperature liquid hydrogen storage is generally used in aerospace or large liquid hydrogen storage and transport ship and other fields. Solid hydrogen storage is a method that uses materials to absorb hydrogen through physical or chemical absorption forming hydrides so as to realize solid storage. Since hydrogen exists in the form of solid hydride, the solid hydrogen storage method has the advantage of high volumetric density (higher than 50 kg H_2 m^{-3}). In addition, the working pressure of solid hydrogen storage is lower (less than 10 MPa) and the

State Grid Jiangsu Electric Power Co, Ltd. Research Institute, Nanjing, Jiangsu, P. R. China. E-mail: vodoco@foxmail.com

purity of hydrogen is higher. Thus, solid hydrogen storage is a good option for hydrogen energy applications.[7,13,14]

As the solid hydrogen storage technology depends heavily on the hydrogen absorption and desorption properties of hydrogen storage materials, the research and development of high-performance hydrogen storage materials is the main topic of the development of solid-state hydrogen storage technology.[7] After decades of development, people have developed a variety of hydrogen storage materials, including hydrogen storage alloys (rare earth-based alloys, titanium-based alloys, *etc.*),[15–19] complex metal hydride (metal alanates,[20–23] metal borohydrides,[24–27] metal nitrides,[28–31] *etc.*), chemical hydrides,[11,32–35] light metal hydrides (magnesium hydride, aluminum hydride, *etc.*),[36–49] absorbents (carbon nanotubes, porous carbon, zeolite, MOFs, *etc.*),[50–53] *etc.* At present, only hydrogen storage alloys have been applied. In general, hydrogen storage alloys consist of one or more hydrogen-loving elements (denoted by A) and one or more hydrogen-repellent elements (denoted by B) and can be denoted by A_mB_n. Elements on the A side mainly contribute to hydrogen storage capacity, while elements on the B side mainly play a catalytic role in regulating the hydrogen absorption and desorption properties of the alloys. According to the difference of element composition and structure, hydrogen storage alloys can be divided into AB_5 ($LaNi_5$ system), AB_2 ($TiMn_2$ system), AB (TiFe system) and A_2B (Mg_2Ni system) types, *etc.*

$TiMn_2$-based alloy is one of the AB_2-type hydrogen storage alloys developed earlier. It is a Laves phase alloy with topological close-packed structure and has a C14 structure ($MgZn_2$-type, hexagonal). Since its discovery in 1970s, $TiMn_2$ alloy has been widely studied, and it is also one of the hydrogen storage material systems that have been applied in practice (Fig. 1). The hydrogen storage capacity of $TiMn_2$ alloy is larger than that of AB_5-type $LaNi_5$ alloy, generally reaching 1.8–2.0 wt%, and it has the characteristics of easy activation (prior hydrogen sorption treatment under certain temperature and hydrogen pressure to remove the oxides or other harmful component), fast hydrogen absorption and desorption, and wide adjustable range of hydrogen absorption and desorption platform pressure. It is thus one of the hot research topics in the field of solid hydrogen storage.

At present, the research on $TiMn_2$ hydrogen storage alloys mainly focuses on the following aspects: (i) improving the activation performance of the alloys and reducing the activation hydrogen pressure; (ii) adjust and control the platform characteristics of hydrogen absorption and desorption to meet the practical application requirements; (iii) increasing the actual hydrogen storage capacity of the alloy; (iv) improve the situation of alloy poisoning. By means of alloy element substitution, composition design, phase and microstructure design, and preparation technology optimization, it is expected to develop $TiMn_2$-based hydrogen storage alloy with easy activation, large hydrogen storage capacity, hydrogen absorption and desorption platform pressure meeting the practical application requirements, and strong anti-poisoning ability. In this work, the research, development and application status of Laves phase $TiMn_2$-based hydrogen storage alloys are reviewed, and the future research and development directions of the $TiMn_2$-based hydrogen storage materials are also discussed.

2 $TiMn_2$-based hydrogen storage alloys

Fig. 2 shows the binary phase diagram of Mn–Ti. There is a wide Laves phase region in the phase diagram, which means that when the stoichiometric ratio of Ti–Mn alloy deviates from $TiMn_2$ obviously, the alloy is still a single Laves phase structure. Among all the Ti–Mn binary alloys, the $TiMn_2$ alloy has a poor hydrogen storage performance, but $TiMn_{1.5}$ has the best hydrogen storage performance, and its room temperature hydrogen storage capacity can reach about 1.8 wt%.

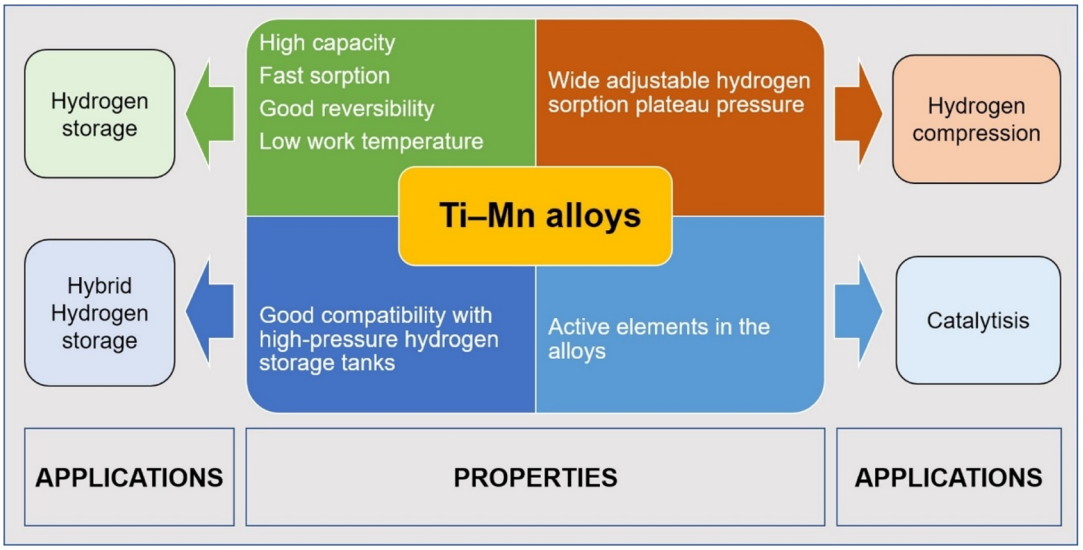

Fig. 1 The hydrogen storage properties, regulation methods and applications of Ti–Mn hydrogen storage alloys.

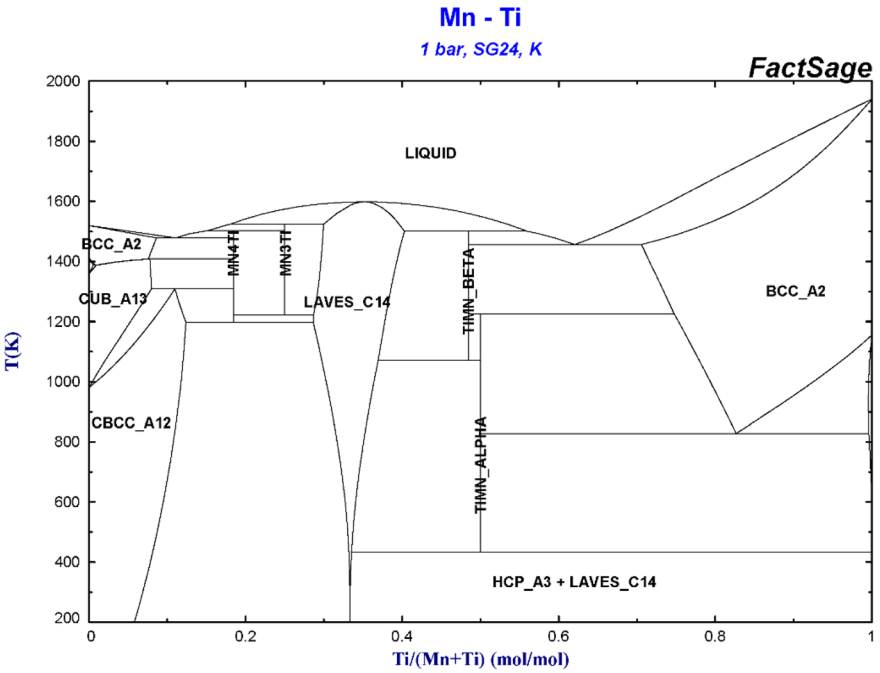

Fig. 2 Binary phase diagram of Mn–Ti.[57,58]

Gamo *et al.*[54] studied the hydrogen storage performance of Ti–Mn binary alloys with different Ti content (33.3 at% to 66.7 at%) at 0–80 °C. It was found that Ti–Mn binary alloys with Ti content less than 36 at% hardly absorb hydrogen at room temperature (the hydrogen absorption pressure is smaller than 4.5 MPa), while the Ti–Mn binary alloys with higher Ti content can react with hydrogen at room temperature without activation treatment. Liang *et al.*[55] think that the reason why $TiMn_{1.5}$ be the best hydrogen storage performance of Ti–Mn binary alloy is that it is located at the titanium-rich edge of Laves phase and deviates from the ideal composition of $TiMn_2$ the most. In addition, Semboshi *et al.*[56] studied the effects of Ti and Mn content on the hydrogen storage performance of binary Ti–Mn alloy. It was found that increasing the volumetric content of $TiMn_2$ phase can improve the hydrogen absorption and desorption performance and the cycle performance of the alloy, while keeping the Mn content as low as possible. The alloy containing 59.4 at% Mn has the best hydrogen absorption and desorption performance, and the capacity decline is the least after many hydrogen absorption and desorption cycles.

In order to regulate the hydrogen storage performance of Ti–Mn alloys, a series of multi-component $TiMn_2$-based hydrogen storage alloys have been developed by partially replacing Ti or Mn elements in $TiMn_2$ alloys with other metal elements, and their performance is better than that of binary alloys. Moriwaki *et al.*[59] replaced Ti by Zr in the $Ti_{1-x}Zr_xMn_2$ ternary alloy and shows that when $0 < x < 0.1$, the alloy does not absorb hydrogen, but with the increase of Zr content, the lattice constant increases and the plateau pressure of hydrogen absorption and desorption decreases. Gamo *et al.*[54] developed four-element and five-element $TiMn_2$-based alloys, in which Ti was partially replaced by Zr, and Mn was replaced by one or two elements of the transition metals Mo, Cu, Co, Ni, Fe, Cr and V. It was found that $Ti_{0.9}Zr_{0.1}Mn_{1.4}V_{0.2}Cr_{0.4}$ had the best hydrogen storage performance among all the alloys studied. In addition, Bobet *et al.*[60] studied alloy $Ti_{0.95}Zr_{0.05}Mn_{1.45}M_{0.5}$ (M = V, Cr, Mn, Co, Ni, Al) and found that at room temperature, the hydrogen storage performance of the alloys where Mn was partially replaced by Cr or V alloy was the best. Chuang *et al.*[61] studied the $Ti_{0.95}Zr_{0.05}Cr_{1.2}Mn_{0.8-x}M_x$ (M = V, Co) multi-component alloy and found that with the increase of V content in the alloy, the hydrogen absorption and desorption plateau pressure of the alloy decreases, but the effect of Co is just the opposite, that is, with the increase of Co content, the hydrogen absorption and desorption plateau pressure of the alloy increases. Zhou *et al.*[62] systematically investigated the hydrogen storage performance of the Ti–Zr–Mn–Cr–V multi-element hydrogen storage alloy. The Ti was partially replaced by Zr and Mn was partially replaced by Cr and V, and the effect of element substitution on microstructure and hydrogen storage performance of the alloy was studied. The results show that with the increase of Zr replacing Ti, the hydrogen storage capacity of the alloy increases gradually, and the platform pressure of hydrogen absorption and desorption decreases sharply. However, with the increase of the ratio of Cr and V replacing Mn, the plateau pressure and hysteresis effect (ratio of the hydrogen absorption to desorption) of hydrogen absorption and desorption of the alloy are obviously improved, but the hydrogen storage capacity decreases slightly.

In a word, compared with other hydrogen storage alloys, $TiMn_2$-based hydrogen storage alloys have better hydrogen storage performance. For example, compared with $LaNi_5$-based alloys, $TiMn_2$-based hydrogen storage alloys have higher hydrogen storage capacity, easier activation and better cycle

performance. After about 10 000 cycles, the hydrogen capacity of $TiMn_2$ binary alloy and multicomponent alloy decreased by 30% and 20%, respectively, and the recycled alloy still maintained the C14 Laves phase structure.[63] The $TiMn_2$-based hydrogen storage alloys received more and more attentions in the scientific research field because of their wide platform pressure and temperature range for hydrogen absorption and desorption and wide application fields.

3 Regulation of the hydrogen storage properties

The hydrogen storage performance of $TiMn_2$-based alloys depends heavily on its composition, structure and preparation technology. In order to obtain $TiMn_2$-based hydrogen storage alloy with excellent comprehensive hydrogen storage performance, researchers have done a lot of research and exploration in the aspects of composition design, structure control and preparation process optimization, and found that the hydrogen storage performance of $TiMn_2$-based hydrogen storage alloy can be improved by partial substitution of alloy elements, ball milling modification, annealing heat treatment and addition of catalyst. The following will introduce the means of controlling the hydrogen storage performance of $TiMn_2$-based alloys.

3.1 Element substitution

The element composition of hydrogen storage alloy generally includes hydrogen-loving elements (denoted by A) and hydrogen-repelling elements (denoted by B). Partial element substitution of A-side element and B-side element is the most commonly used and effective means to regulate the hydrogen storage performance of alloy.

In order to improve the hydrogen absorption and desorption performance, enhance the activation performance and reduce the hysteresis effect of $TiMn_2$-based hydrogen storage alloys, transition metal elements were commonly used to partially replace the elements on the A and B sides, and adjust the proportion of elements, so as to regulate the hydrogen storage performance of $TiMn_2$-based alloys.

For the substitution of A-side elements, Zr, Hf, Sc and other elements are generally used to replace part of Ti elements in the alloy. The results show that Zr can change the affinity of hydrogen and alloy, and increase the lattice constant of alloy crystal, which can effectively reduce the pressure of hydrogen absorption and discharge platform, improve the slope of platform and the hydrogen storage performance of alloy.[64,65] It has been proved by Moriwaki *et al.*[59] that by changing the Ti/Zr ratio, the platform pressure, hysteresis and platform inclination rate of $TiMn_2$-based alloy can also be improved. Pickering *et al.*[66] found that when the Zr/(Ti + Zr) ratio is low, the PCT properties of the material can be controlled in a large range by changing the V content, thus improving the hydrogen storage capacity. In addition, replacing Ti with a small amount of Sc can significantly improve the hydrogen storage capacity and activation performance, and at the same time reduce the platform pressure of hydrogen absorption and desorption, but the slope factor increases.[67,68]

As for the substitution of the B-side elements, transition metal elements such as Cr, Fe, V, Co, W, Ni, Cu, Mo, and other elements such as Si and Al are usually used to partially replace Mn in the $TiMn_2$-based alloy. It was found that Cr element can effectively reduce the hysteresis effect of hydrogen absorption and desorption platform of $TiMn_2$-based alloy. The hydrogen absorption and desorption platform become shorter, and the unit cell volume of the alloy increases, but the hydrogen absorption capacity decreases. When the Cr/Mn ratio increases, the hydrogen absorption and desorption platform become shorter, the slope of the platform increases, and the hydrogen absorption capacity decreases.[59,64,69] Xu *et al.*[70] studied the $Ti_{0.8}Zr_{0.2}Mn_{2-x}Cr_x$ ($x = 0.2$, 0.4, 0.6, 0.8, 1.0) alloy and showed that the hydrogen absorption capacity of the alloy increases with the increase of Cr content, and the activation performance of the alloy is improved when $x > 6$. Cu can make the pressure of hydrogen absorption and desorption platform of $TiMn_2$-based alloy flatter, but the hydrogen storage capacity decreases. The element V can effectively reduce the pressure of the hydrogen absorption and desorption platform without reducing the hydrogen storage capacity of $TiMn_2$-based alloy and make the lag of the pressure of the hydrogen absorption and desorption platform smaller.[61,64,71] Partial substitution of Mn by Co element can increase the plateau pressure of hydrogen absorption and desorption of $TiMn_2$-based alloy, and with the increase of Co element content, the plateau pressure increases.[61] It has been found that adding a small amount of Mo can increase the hydrogen storage capacity of $TiMn_2$-based alloy. For example, Au *et al.*[71] studied the alloys $Ti_{0.8}Zr_{0.3}Mn_{1.5}V_{0.2}Cr_{0.2}$ and $Ti_{0.8}Zr_{0.3}Mn_{1.4}Mo_{0.1}V_{0.2}Cr_{0.2}$, and found that replacing Mn with a small amount of Mo can increase the hydrogen storage capacity of $TiMn_2$-based alloys. But when Gamo *et al.*[54] was studying the $Ti_{0.8}Zr_{0.2}Mn_{2-y}Mo_y$, they found that when Mo element partially replaced Mn element, with the increase of Mo element content, the hydrogen absorption and desorption platform pressure of the alloy increase and the hydrogen storage capacity decrease, which was contrary to the above results. Therefore, the effect of Mo element replacing Mn element on the hydrogen storage performance of $TiMn_2$-based alloy needs further research and verification. Replacing Mn element on B side with Ni element can flatten the hydrogen absorption and desorption platform of PCT curve of $TiMn_2$-based alloy and increase the platform pressure.[72] However, replacing Mn with Al can reduce the hydrogen absorption and desorption platform pressure of $TiMn_2$-based alloy, and at the same time, the hydrogen storage capacity will be greatly reduced.[60,73] In addition, Au *et al.*[71] also proved that replacing Mn with Si and Al will reduce the hydrogen storage capacity of $TiMn_2$-based alloy but will increase the pressure of hydrogen absorption and desorption platform. The substitution of Mn by Co, W and other elements can improve the PCT curve characteristics of $TiMn_2$-based alloy and flatten the curve, but the hydrogen storage capacity decreases, and the plateau pressure of the alloy easily increases. In the alloy–hydrogen system containing Fe and V, the hysteresis decreases, but the hydrogen

storage capacity decreases.[69] However, Xu *et al.*[70] found that when V–Fe alloy is used instead of pure V in the Ti–Zr–Mn–V–M series alloys, the hydrogen absorption capacity of the alloy hardly decreases. Increasing the contents of Zr and Mn in Ti–Zr–Fe–Mn alloys at the same time will reduce the pressure of hydrogen absorption and desorption platform.[74] Hong *et al.*[75] explored the substitution effect of a large number of metal elements on the Mn element on the B side of $Ti_{0.8}Zr_{0.2}Mn_{1.5}M_{0.5}$ (M = Ti, V, Fe, Co, Ni, Cu, Al, Nb and Mo, *etc.*) alloy in order to improve the comprehensive hydrogen storage performance of $TiMn_2$-based alloy. It was found that V, Cr, Fe and Cu are the most ideal substitution elements, especially Cr, whose $Ti_{0.8}Zr_{0.2}Mn_{1.5}Cr_{0.5}$ shows the best performance. Regarding the hysteresis, Hagström *et al.*[76] proved by experiments that there is an experimental correlation between the different volume expansion of coexisting phases and the hysteresis of hydrogen absorption and desorption of the alloy, which indicates that the volume expansion of the alloy has a great influence on the hysteresis of the hydrogen absorption and desorption platform.

3.2 Ball milling modification

High-energy ball milling can crush the particles of hydrogen storage alloy to micron or nanometer level, which can increase the contact area between hydrogen storage alloy and hydrogen. At the same time, it can clear the surface pollution layer of the original alloy to a certain extent, and make the alloy produce a large number of fresh surfaces, thus facilitating the adsorption and diffusion of hydrogen. In addition, ball milling is also an effective means of mechanical alloying, and new alloys can be prepared by this technology. Therefore, high-energy ball milling can be used to modify $TiMn_2$-based alloy to improve its hydrogen storage performance. Amorphous phase will be formed in $TiMn_2$-based alloy after ball milling.[77] Chen *et al.*[78] systematically studied the phase structure and hydrogen storage performance of $Ti_{0.9}Zr_{0.1}Mn_{1.5}$ hydrogen storage alloy after ball-milling modification. It was found that ball-milling modification did not change the phase structure of the alloy, and proper ball-milling modification could effectively improve the comprehensive hydrogen storage performance of $Ti_{0.9}Zr_{0.1}Mn_{1.5}$ alloy.

3.3 Annealing heat treatment

For the as-melted alloy, heat treatment can reduce or even eliminate the intergranular segregation and lattice stress. Heat treatment is also often used to improve the hydrogen absorption and desorption performance of hydrogen storage alloys. After heat treatment, the grain size of the hydrogen storage alloy is refined, the internal stress is reduced or eliminated, and the structural defects of the alloy are reduced, thus the activation performance, cycle stability and hydrogen storage capacity are improved.[79] Liu *et al.*[64] annealed the $TiMn_2$-based hydrogen storage alloy to improve the platform tilt rate of the alloy. Generally speaking, the platform tilt of hydrogen storage alloys is caused by macroscopic micro-segregation and microscopic chemical energy and strain energy effects, and the effect of micro-segregation can be reduced by annealing heat treatment.[80] As we all know, the slope of hydrogen absorption and desorption platform of hydrogen storage alloy is partly due to the uneven composition of the alloy, which can be mostly eliminated by annealing heat treatment. The research of Bobet *et al.*[73] shows that the annealing process leads to the disappearance of the secondary phase, thus making the compound more and more uniform and the slope smaller. Huang *et al.*[81] found that after heat treatment, the second phase will precipitate in the $TiMn_2$-based hydrogen storage alloy, the microstructure of the alloy will be improved, the hydrogen absorption and desorption performance will be improved, and the enthalpy change, and entropy change of hydrogen absorption and desorption will decrease. Qian *et al.*[82] carried out homogenization annealing treatment on $TiMn_x$ alloy and found that the amount of hydrogen absorption and desorption was larger than that without annealing treatment, and the plateau became flat, which indicated that annealing treatment could significantly improve the hydrogen storage performance of the alloy. Jiang *et al.*[83] studied the effect of heat treatment on the properties and microstructure of sub-stoichiometric $TiMn_2$-based hydrogen storage alloys. The results showed that heat treatment increased the hydrogen storage capacity of $TiMn_2$-based hydrogen storage alloys, widened the hydrogen absorption and desorption platform, but also increased the slope of the platform.

However, in some studies, annealing heat treatment did not significantly improve the properties of $TiMn_2$-based hydrogen storage alloys. Komazaki *et al.*[74] studied the effect of annealing on PCT curve of Ti–Zr–Fe–Mn based alloy and found that annealing did not improve the tilt rate of the platform. In addition, Park *et al.*[80] also got this conclusion when studying Ti–Zr–Mn–Cr based alloys and believed that the tilt of platform pressure was caused by chemical energy or strain energy effect. However, in most cases, heat treatment does improve the microstructure of $TiMn_2$-based hydrogen storage alloys, eliminate the microscopic internal stress, and thus improve the hydrogen storage performance of the alloys.

3.4 Additive modification

Adding a small amount of other kinds of alloys into $TiMn_2$-based hydrogen storage alloy by ball milling to form hydrogen storage composite can effectively improve the hydrogen storage performance of the alloy. For example, Chu *et al.*[84] added a small amount of La–Mg-based alloy to $Ti_{0.9}Zr_{0.2}Mn_{1.5}Cr_{0.3}V_{0.3}$ alloy and made the composite by mechanical ball milling. It was found that after adding La–Mg-based alloy and ball milling for 2 h, the original C14 Laves phase structure of the composite was maintained, the hydrogen absorption and desorption kinetics was obviously improved, and the hydrogen absorption and desorption platform pressure decreased, which was due to the high dispersion of La–Mg-based alloy and the acceleration of the introduction of microcracks after ball milling.

3.5 Influence of impurities

If the hydrogen contains impurity gas, it will affect the hydrogen storage performance of $TiMn_2$-based alloy. Impurity gases can be divided into two categories according to the influence degree: (1)

N_2 or CH_4, *etc.* These gases only change the hydrogen absorption kinetics of $TiMn_2$-based hydrogen storage alloys, but have little effect on the hydrogen storage capacity of the alloys; (2) O_2, CO, CO_2 or H_2O, *etc.* If there is a small amount of these impurity gases in hydrogen, the hydrogen storage capacity of $TiMn_2$-based system will be reduced, and the cycle stability will be deteriorated.

Block *et al.*[85] studied the influence of a small amount of CO and CH_4 mixed gas in hydrogen on the hydrogen storage performance of $TiMn_2$-based alloy. It was found that the presence of a small amount of CH_4 (5%) in hydrogen can reduce the hydrogen absorption kinetic performance of the alloy, but the reversible hydrogen storage capacity remains unchanged. However, the presence of a small amount of CO in hydrogen will passivate the alloy after many hydrogen absorption and desorption cycles, which is because CH_4 will be slightly physically adsorbed on the surface of $TiMn_2$-based alloy. Therefore, the absorption rate of hydrogen by the alloy is slowed down, but when the hydrogen storage alloy is released under the vacuum condition of 2 Pa, CH_4 can be desorbed again, thus avoiding the accumulation of CH_4 damage to the alloy. The effect of CO on the hydrogen storage performance of $TiMn_2$-based alloy is that CO will be adsorbed on the surface of $TiMn_2$ alloy, but it will be desorbed very little in the process of hydrogen desorption. Therefore, with the increase of cyclic hydrogen absorption and desorption times, the amount of CO adsorbed on the surface of the alloy will gradually increase, thus the hydrogen absorption capacity of the alloy will gradually decrease. Morita *et al.*[86] studied the effects of nonmetallic elements B, C, O, S and Se on the hydrogen storage performance of $Ti_{0.9}Zr_{0.1}Mn_{1.4}Cr_{0.4}V_{0.2}$ alloy. The results showed that the addition of nonmetallic elements S, Se and C greatly increased the platform pressure of the alloy, increased the slope coefficient of the platform, and expanded the pressure hysteresis. The plateau slope coefficient of $TiMn_2$-based alloy is usually improved by heat treatment, while the plateau slope coefficient can be improved without heat treatment by adding nonmetal.

3.6 Phase structure control

The comprehensive performance of single-phase hydrogen storage alloy is better than that of multiphase hydrogen storage alloy, because the existence of multiphase easily leads to the appearance of double platforms in the PCT curve, which is not conducive to practical application, and the existence of impurity phase or segregation phase easily leads to the increase of PCT curve hysteresis coefficient.[87] Kazemipour *et al.*[88] proved that the kinetic properties of hydrogen absorption and desorption and hydrogen storage capacity of the alloy are affected by the amount and proportion of existing phases.

In a word, $TiMn_2$-based alloy has higher hydrogen storage capacity than rare earth alloy, easier activation than TiFe alloy, faster hydrogen absorption and desorption, wide adjustable range of hydrogen absorption and desorption platform pressure and good cycle stability. So, it is a kind of hydrogen storage material with great application prospect. By means of element substitution, ball milling modification, heat treatment, microstructure control, impurity gas control, additive modification, *etc.*, the high-performance $TiMn_2$-based hydrogen storage alloy can be developed to meet the practical requirements. Table 1 lists the hydrogen storage properties of some selected $TiMn_2$-based hydrogen storage alloys.

4 Application of $TiMn_2$-based hydrogen storage alloy

Compared with rare earth-based alloys, $TiMn_2$-based alloys have higher hydrogen storage capacity (up to 2 wt%), easy activation, fast hydrogen absorption and desorption rate and good toxicity resistance. Therefore, $TiMn_2$-based alloys can be used for high-density hydrogen storage, especially for stationary hydrogen storage with high volumetric hydrogen storage density. In addition, the pressure of the hydrogen absorption and desorption platform of $TiMn_2$-based alloy can be adjusted in a wide range (several to dozens MPa), which determines that $TiMn_2$-based alloy can be used for static compression of hydrogen and can also be used for high pressure-metal hydride hybrid hydrogen storage. Finally, $TiMn_2$-based alloys contain some transition metal elements, which are active catalytic components for many hydrogen storage materials. Therefore, $TiMn_2$-based alloys can also be used as catalysts or additives for some hydrogen storage materials. The following will introduce some applications of $TiMn_2$-based alloys.

Table 1 Hydrogen storage properties of various $TiMn_2$-based alloys

Alloys	C_{max}[a] (wt%)	P_a[b] (MPa)	P_d[c] (MPa)	H_f[d]	S_f[e]	Ref.
$Ti_{1.06}Cr_{1.3}Mn_{0.2}Fe_{0.5}$	1.83	—	2.5 (−30 °C)	0.33	0.72	89
$(Ti_{0.8}Zr_{0.2})_{1.1}Mn_{1.2}Cr_{0.55}Ni_{0.2}V_{0.05}$	1.82	1.1 (25 °C)	0.4 (25 °C)	0.93	0.37	90
$Ti_{0.95}Zr_{0.05}Mn_{0.9}Cr_{0.9}V_{0.2}$	1.78	2.6 (30 °C)	2.3 (30 °C)	0.14	—	62
$Ti_{0.90}Sc_{0.10}Mn_{1.4}V_{0.6}$	2.11	0.4 (20 °C)	0.2 (20 °C)	0.69	0.46	67
$Ti_{30}V_{15.8}Mn_{49.4}(Zr_{0.5}Cr_{1.1}Fe_{2.9})$	1.60	4.4 (26 °C)	2.4 (26 °C)	0.57	0.23	91
$Ti_{0.78}Sc_{0.22}MnCr$	1.90	0.3 (20 °C)	0.2 (20 °C)	0.47	2.1	68
$Ti_{0.68}Zr_{0.32}MnCr$	1.90	0.3 (20 °C)	0.2 (20 °C)	0.47	1.5	65
$Ti_{0.95}Zr_{0.15}Mn_{1.1}Cr_{0.7}V_{0.2}$	2.80 (atomic ratio)	0.9 (20 °C)	0.7 (20 °C)	0.21	—	92
$(Ti_{0.8}Zr_{0.2})_{1.05}Mn_{0.8}Cr_{1.05}V_{0.05}Cu_{0.1}$	1.90	0.3 (30 °C)	0.2 (30 °C)	0.41	—	80
$Ti_{0.9}Zr_{0.2}Mn_{1.6}Ni_{0.2}V_{0.2}$	2.10	0.6 (25 °C)	0.3 (25 °C)	0.80	1.27	70

[a] C_{max} is the maximum hydrogen storage capacity. [b] P_a is the hydrogen absorption plateau pressure. [c] P_d is the hydrogen desorption plateau pressure. [d] H_f is the plateau hysteresis which is calculated by $\ln(P_a/P_d)$. [e] S_f is the slope of the hydrogen desorption plateau which is calculated by $d(\ln P)/d(H\ wt\%)$.

4.1 Hydrogen storage

Among the many Ti-based alloys, $TiMn_2$-based alloys have high hydrogen storage capacity and relatively suitable platform pressure and are one of the most suitable candidate alloys for high-density hydrogen storage devices.

General Research Institute for Nonferrous Metals developed an external circulating heat exchange metal hydride solid hydrogen storage tank[93] (Fig. 3). The solid hydrogen storage tank adopts horizontal cylindrical, which is divided into two layers with the outermost is heat transfer layer. The heat transfer layer is set inside the annular diversion structure. The loop diversion structure not only increase the heat exchange area, but also increases the heat transfer medium (water) in heat transfer layer in the process, which further improves the thermal efficiency. The solid hydrogen storage tank has an outer diameter of 150 mm and a total length of 1500 mm. The hydrogen storage alloy used is $TiMn_2$-based alloys, which is about 55 kg and has an effective hydrogen storage capacity of 12 N m^3. At 65 °C, the hydrogen storage tank can stably provide 11.2 N m^3 at a hydrogen discharge rate of 50 SL min^{-1}.

Metal hydride hydrogen storage system can be designed with flexibility, customizability and modularization according to the actual application scenarios and scales. In order to further improve the application flexibility of metal hydride hydrogen storage system, General Research Institute for Nonferrous Metals developed a modular hydrogen storage device, as shown in Fig. 4, with an effective hydrogen storage capacity of 44 N m^3. The hydrogen storage device is composed of four 11 N m^3 hydrogen storage tanks. The adopted hydrogen storage material is $TiMn_2$-based hydrogen storage alloy, and each hydrogen storage tank adopts external heat exchange mode. The hydrogen storage device has excellent hydrogen releasing performance. At 60 °C, the hydrogen storage system can stably release hydrogen at 75 SL min^{-1} and provide a capacity of 43.4 N m^3.

4.2 Hydrogen compression

According to the thermodynamic properties of hydrogen storage alloys, it can be known from the van't Hoff equation that the equilibrium hydrogen pressure of hydrogen storage alloys increases with the increase of temperature. Therefore, this characteristic of hydrogen storage alloys can be used to realize the compression and pressurization of hydrogen. Specifically, the hydrogen absorption and desorption platform pressure can be increased by increasing the working temperature of the hydrogen storage alloy, or by increasing the hydrogen absorption and desorption platform pressure through adjusting the composition of the hydrogen storage alloy. Hydrogen compression with hydrogen storage alloy is an effective and reliable method. Compared with the traditional mechanical hydrogen compression, this method has many advantages, including quietness, reliable safety, environmental friendliness, efficient hydrogen purification and low maintenance cost.[94,95]

$TiMn_2$-based alloy is suitable for the integrated storage and compression of hydrogen because of its good hydrogen absorption and desorption cycle performance, high hydrogen storage capacity, easy activation, good poisoning resistance, relatively low cost and wide adjustable range of hydrogen absorption and desorption platform. Klyamkin *et al.*[96] found that the plateau pressure of hydrogen absorption and desorption of $TiMn_2$-based alloy can even reach hundreds of atmospheres. Peng *et al.*[89] designed a three-stage metal hydride compressor for hydrogen refueling station, as shown in Fig. 5. By using Ti–Cr–Mn–Fe hydrogen storage alloy, 85 MPa hydrogen pressurization can be achieved. Galvis E *et al.*[97] also designed a three-stage metal-hydride compressor using three different types of AB_2-type $TiMn_2$-based alloys. Guo *et al.*[98] developed Ti–Mn and Ti–Cr alloys as the low-pressure and high-pressure hydrogen storage material for a two-stage metal hydride hydrogen compressor. These two alloys were optimized to be $Ti_{0.9}Zr_{0.1}Mn_{1.4}Cr_{0.35}V_{0.2}Fe_{0.05}$ and $TiCr_{1.55}Mn_{0.2}Fe_{0.2}$. The combination of these two alloys can increase the hydrogen pressure from 4 MPa to 100 MPa with hot oil as the heating medium. Nayebossadri *et al.*[91] developed a high-pressure $TiMn_2$-based alloy $TI_{30}V_{15.8}Mn_{49.4}$ $(Zr_{0.5}Cr_{1.1}Fe_{2.9})$ for a two-stage hydrogen compression, which was able to compress hydrogen from 1.5 MPa to over 35 MPa. And the operating temperature does not exceed 130 °C. Guo *et al.*[98] adopted $Ti_{0.9}Zr_{0.1}Mn_{1.4}Cr_{0.35}V_{0.2}Fe_{0.05}$ alloy to increase the hydrogen pressure from 4 MPa to 20 MPa below 128 °C. Wang *et al.*[92] used

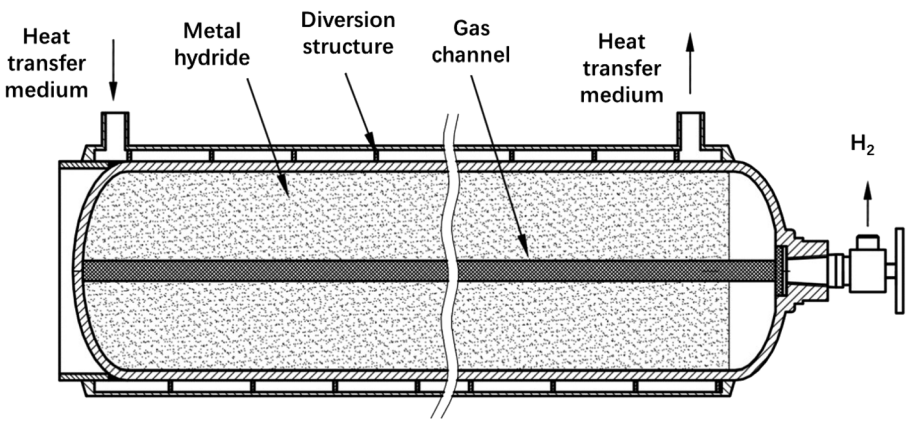

Fig. 3 A hydrogen storage tank with external heat transfer structure.[93]

Fig. 4 A hydrogen storage system with modularized structure.

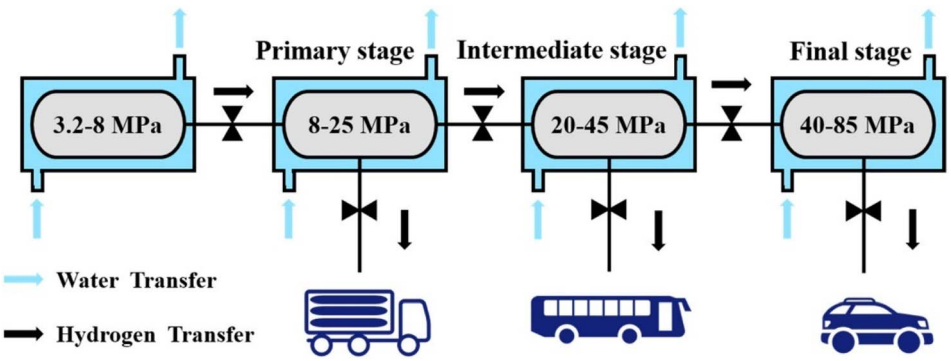

Fig. 5 Diagram displaying a three-stage metal hydride hydrogen compressor.[89]

the Ti–Mn multicomponent alloys for a two-stage thermal driven chemical hydrogen compressor with a hydrogen capacity of 50 L. They used water as the heat exchange medium and compress the hydrogen from 2.5 MPa to more than 40 MPa.

4.3 High pressure-solid state hybrid hydrogen storage

High-pressure gaseous hydrogen storage has the advantages of fast and convenient hydrogen charging and discharging, especially the good dynamic response ability of hydrogen discharging, but its volume hydrogen storage density is low, and it takes up a large space. However, solid-state hydrogen storage has the advantages of high volumetric hydrogen storage density and good safety, but its dynamic response to hydrogen charging and discharging is poor. If high-pressure gaseous hydrogen storage and solid hydrogen storage are combined, the advantages of the two hydrogen storage methods can be fully exerted. Therefore, people have developed a high-pressure and solid hybrid hydrogen storage method, the working pressure of which is generally above 20 MPa, and the hydrogen storage alloys with high plateau pressure are used as the hydrogen storage materials.

In order to develop a hydrogen storage alloy for a 35 MPa hybrid hydrogen storage containers, Shibuya *et al.*[99] synthesized a $TiMn_2$-based AB_2-type alloy $Ti_{0.5}V_{0.5}Mn$ suitable for hybrid hydrogen storage containers by adding V as a third element to the Ti–Mn binary alloy. The hydrogen absorption capacity of the alloy is 1.8 wt% at 7 MPa H_2 and −30 °C. The capacity is not saturated at such conditions. The hydrogen storage capacity can be continued to be increased to a certain extent until the hydrogen pressure reaches 35 MPa, which is the working pressure of the hybrid hydrogen storage containers.

In addition to the research of hybrid hydrogen storage containers for automotive applications, $TiMn_2$-based alloys have also been applied to the low-pressure hybrid hydrogen storage of fuel cell electric bicycles. For example, Tu *et al.*[90] obtained the optimal alloy composition $(Ti_{0.8}Zr_{0.2})_{1.1}$-$Mn_{1.2}Cr_{0.55}Ni_{0.2}V_{0.05}$ by progressively replacing the Ti–Zr–Cr based alloy with Mn, Ni and V and had a hydrogen storage capacity of 1.82 wt% at 25 °C. The hydrogen absorption pressure is 1 MPa, and the hydrogen desorption pressure is 0.4 MPa. With rapid hydrogen absorption kinetics and low hydrogen

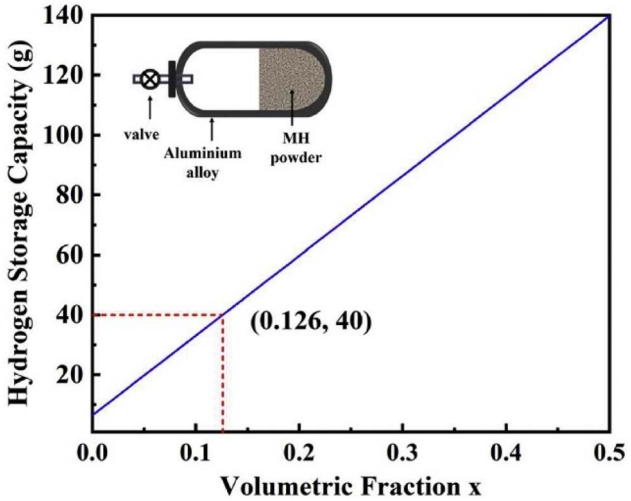

Fig. 6 Relationship between the hydrogen storage capacity and the volume of the filled alloys in a 4 MPa low-pressure hybrid tank.[90]

absorption and desorption platform, it is suitable for the low-pressure hybrid hydrogen storage tank of fuel cell electric bicycle. They also calculated the hydrogen storage capacity of a 2 L aluminum tank. Without filling hydrogen storage alloy, the hydrogen storage capacity is 6.3 g of hydrogen at room temperature and 4 MPa hydrogen pressure. Under the same conditions, the hydrogen storage capacity will be greatly increased when the hydrogen storage alloy is partially filled. Fig. 6 shows the relationship between the hydrogen storage mass in the hybrid hydrogen storage tank and the volume ratio of hydrogen-filling alloy. It can be seen that when hydrogen storage alloy is filled into the tank, the hydrogen storage capacity of the hybrid hydrogen storage tank is greatly improved. When half the volume of the hybrid hydrogen storage tank is filled with hydrogen storage alloy, the tank can store 140 g of hydrogen.

Liu *et al.*[100] developed a gas–solid hybrid hydrogen storage device for a 10 kW hydrogen energy storage test platform, shown in Fig. 7. Its working pressure was only 5 MPa, and the $TiMn_2$-based hydrogen storage alloy was used as the hydrogen storage material, with an effective hydrogen storage capacity of 1.7 wt%. Through the optimization of the proportion of gaseous hydrogen and solid hydrogen, a hybrid hydrogen storage device with a hydrogen storage capacity of 12 N m^3 and a volume hydrogen storage density of 40 kg H_2 m^{-3} was designed. The hydrogen storage device can supply hydrogen stably for 14.8 min at a temperature as low as −15 °C and a flow rate of 100 SLM, with excellent low-temperature hydrogen desorption capacity. It can meet the cold start requirements of fuel cells.

4.4 $TiMn_2$-based alloy as additive

The hydrogen storage materials with excellent comprehensive properties can be obtained by combining two kinds of hydrogen storage materials. For example, the hydrogen storage performance of a composite combining the Ti–Mn based alloy and Ti–V based alloy by ball milling was significantly improved. Kumar *et al.*[101] explored the hydrogen storage performance of $Ti_{0.32}Cr_{0.43}V_{0.25}$ alloy and its composite materials with $TiMn_2$. The research results show that, compared with pure $Ti_{0.32}Cr_{0.43}V_{0.25}$ alloy, with the increase of $TiMn_2$ content, the hydrogen absorption and desorption platform of the composite increases, the width of the platform area decreases, and the hydrogen release temperature decreases. In addition, the initial hydrogen absorption kinetics performance is better, but the hydrogen absorption capacity drops sharply. Chen *et al.*[78] added 10 wt% of $Ti_{0.9}Zr_{0.1}Mn_{1.5}$ to $Ti_{9.6}V_{86.4}Fe_4$ by ball milling to form a composite. The composite is composed of BCC main phase and C14 Laves second phase. The activation performance and effective hydrogen release amount of the alloy have been greatly improved, and the platform characteristics have also been significantly improved, but the hydrogen storage capacity of the alloy has decreased. Zhao *et al.*[102] found that the platform pressure of the $LaNi_5$ + x wt% $TiMn_{1.19}$ composite can be effectively reduced with the increase of the content of $TiMn_{1.19}$.

Ti–Mn based alloys can also be made into nanocomposites with new hydrogen storage materials such as MgH_2, thereby

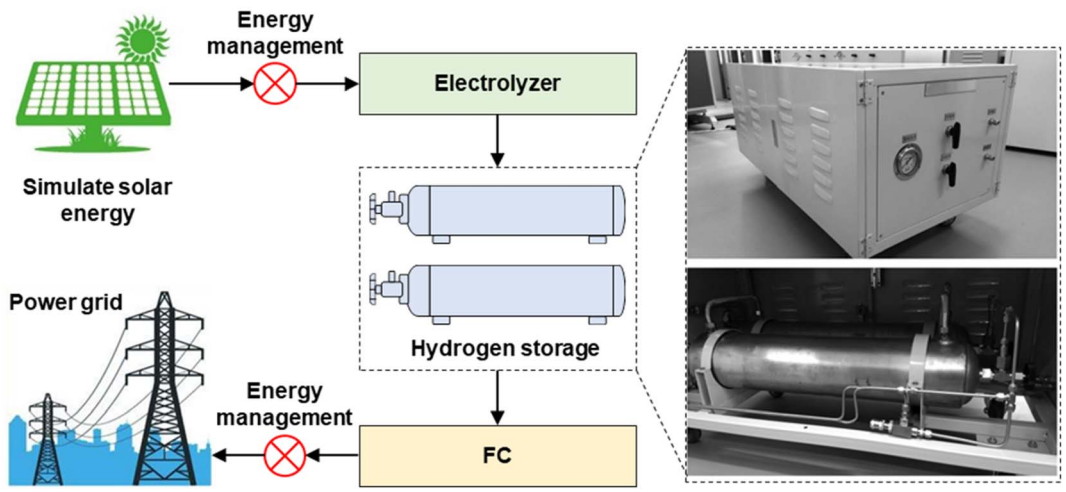

Fig. 7 A gas–solid hybrid hydrogen storage device for a 10 kW hydrogen energy storage test platform.[100]

regulating the hydrogen storage performance of MgH_2. El-Eskandarany *et al.*[103] used 10 wt% $TiMn_2$ intermetallic compound nano-powder as a catalyst to dope MgH_2 nano-powder, and obtained good hydrogen absorption performance and fast hydrogen absorption rate. The time required to absorb/desorb 5.8 wt% H_2 at 225 °C is 150 s and 500 s respectively. In addition, the nanocomposites have good cycling performance. At a lower temperature of 225 °C, the capacity does not have serious attenuation after 414 consecutive cycles. Hu *et al.*[104,105] studied the catalysis of $TiMn_{1.5}$ amorphous alloy in Mg hydrogenation process and prepared a Mg + 30 wt% $TiMn_{1.5}$ nano/amorphous composites by high-energy reaction ball milling. They found that $TiMn_{1.5}$ amorphous alloy can refine Mg particles, and effectively dissociate hydrogen molecules, providing two different stages of "fast channels" for hydrogen atom diffusion. The composites have good hydrogen absorption and desorption kinetics and a reduced hydrogen release temperature of MgH_2. Dai *et al.*[106] studied the stability and hydrogen absorption performance of $TiMn_2$ surface and $Mg/TiMn_2$ interface system using the first principle calculation method and found that inserting MgH_2 in to the $TiMn_2$ layer can greatly improve the hydrogen absorption performance of Mg, which will expand the practical application potential of Mg as a hydrogen storage medium. Khodaparast *et al.*[107] prepared a composite consisting of MgH_2 + 5 at% Ti–Mn–Cr by mechanically milling MgH_2 powder and Ti–Mn–Cr based alloy powder synthesized by electric arc furnace melt spinning. The dehydrogenation temperature of MgH_2 was reduced from 399 °C to 345 °C. Fan *et al.*[108] prepared Mg + x wt% ($Ti_{0.9}Zr_{0.2}Mn_{1.5}Cr_{0.3}$) ($x$ = 20, 30, 40) composites by hydrogen reaction ball milling and explored their hydrogen absorption kinetics. They found that with the increase of alloy content, the hydrogen absorption kinetics of the composites accelerated, its catalytic effect was good, and it can also rapidly absorb hydrogen at a lower temperature, and with the increase of temperature, the hydrogen absorption kinetics became better. In addition, Ti–Mn based alloys can also be used as the matrix to synthesize MgH_2 at low temperatures. For example, Orimo *et al.*[109] took $Ti_{0.6}Zr_{0.4}Mn_{0.8}CrCu_{0.2}$ as the matrix and Mg as the raw material. After annealing heat treatment, MgH_2 can be synthesized after multiple hydrogen absorption and desorption cycles at 100 °C and 1 MPa hydrogen pressure.

5 Summary and prospect

Among many hydrogen storage material systems, Ti–Mn hydrogen storage alloy is one of the few hydrogen storage material systems that can be put into practical use. Ti–Mn hydrogen storage alloys have the characteristics of relatively high hydrogen storage capacity, easy activation, fast hydrogen absorption and desorption rate, wide adjustable range of hydrogen absorption and desorption platform pressure, and good cycle performance, *etc.* They are the key research directions in the field of solid hydrogen storage. Because the gravimetric hydrogen storage density of Ti–Mn hydrogen storage alloy is still low for on-board application, Ti–Mn hydrogen storage alloy is more suitable for stationary scene. In fact, Ti–Mn hydrogen storage alloys have been well applied in the fields of high-density storage of hydrogen and static compression of hydrogen. Hydrogen storage system based on Ti–Mn hydrogen storage alloys have been applied in the field of hydrogen generation from renewable energy and also in the integrated storage and compression of hydrogen in hydrogen refueling stations.

In the future, regarding the research and development and application of Ti–Mn hydrogen storage alloys, the following aspects need to be considered: (i) accurate design of Ti–Mn hydrogen storage alloys and customized control of hydrogen storage properties; (ii) technical problems of batch preparation of Ti–Mn hydrogen storage alloys; (iii) efficient heat and mass transfer design of solid hydrogen storage tank based on Ti–Mn hydrogen storage alloy; (iv) cost reduction. It is believed that the Ti–Mn hydrogen storage alloys will play an important role in the large-scale application of hydrogen energy.

Conflicts of interest

There are no conflicts to declare.

Acknowledgements

Dr Peng Xiao thanks the project support from State Grid Jiangsu Electric Power Co., Ltd. (J2021175).

References

1 Y. Zhang, L. Wang, N. Wang, L. Duan, Y. Zong, S. You, F. Maréchal, J. Van herle and Y. Yang, *Renewable Sustainable Energy Rev.*, 2019, **116**, 109465.
2 D. Apostolou and P. Enevoldsen, *Renewable Sustainable Energy Rev.*, 2019, **112**, 917–929.
3 D. Parra, L. Valverde, F. J. Pino and M. K. Patel, *Renewable Sustainable Energy Rev.*, 2019, **101**, 279–294.
4 M. Ozturk and I. Dincer, *Int. J. Hydrogen Energy*, 2021, **46**, 31511–31522.
5 T. Egeland-Eriksen, A. Hajizadeh and S. Sartori, *Int. J. Hydrogen Energy*, 2021, **46**, 31963–31983.
6 Z.-X. Yang, X.-G. Li, Q.-L. Yao, Z.-H. Lu, N. Zhang, J. Xia, K. Yang, Y.-Q. Wang, K. Zhang, H.-Z. Liu, L.-T. Zhang, H.-J. Lin, Q.-J. Zhou, F. Wang, Z.-M. Yu and J.-M. Ma, *Rare Met.*, 2022, **41**, 3251–3267.
7 L. Schlapbach and A. Zuttel, *Nature*, 2001, **414**, 353–358.
8 J. Zheng, X. Liu, P. Xu, P. Liu, Y. Zhao and J. Yang, *Int. J. Hydrogen Energy*, 2012, **37**, 1048–1057.
9 R. von Helmolt and U. Eberle, *J. Power Sources*, 2007, **165**, 833–843.
10 A. Sarkar and R. Banerjee, *Int. J. Hydrogen Energy*, 2005, **30**, 867–877.
11 D. Berstad, S. Gardarsdottir, S. Roussanaly, M. Voldsund, Y. Ishimoto and P. Nekså, *Renewable Sustainable Energy Rev.*, 2022, **154**, 111772.
12 G. Arnold and J. Wolf, *Teion Kogaku*, 2005, **40**, 221–230.
13 B. Sakintuna, F. Lamari-Darkrim and M. Hirscher, *Int. J. Hydrogen Energy*, 2007, **32**, 1121–1140.

14 A. Zuttel, *Naturwissenschaften*, 2004, **91**, 157–172.
15 J.-M. Joubert, V. Paul-Boncour, F. Cuevas, J. Zhang and M. Latroche, *J. Alloys Compd.*, 2021, **862**, 158163.
16 A. B. Aybar and M. Anik, *J. Energy Chem.*, 2017, **26**, 719–723.
17 M. Hirscher, V. A. Yartys, M. Baricco, J. Bellosta von Colbe, D. Blanchard, R. C. Bowman, D. P. Broom, C. E. Buckley, F. Chang, P. Chen, Y. W. Cho, J.-C. Crivello, F. Cuevas, W. I. F. David, P. E. de Jongh, R. V. Denys, M. Dornheim, M. Felderhoff, Y. Filinchuk, G. E. Froudakis, D. M. Grant, E. M. Gray, B. C. Hauback, T. He, T. D. Humphries, T. R. Jensen, S. Kim, Y. Kojima, M. Latroche, H.-W. Li, M. V. Lototskyy, J. W. Makepeace, K. T. Møller, L. Naheed, P. Ngene, D. Noréus, M. M. Nygård, S.-i. Orimo, M. Paskevicius, L. Pasquini, D. B. Ravnsbæk, M. Veronica Sofianos, T. J. Udovic, T. Vegge, G. S. Walker, C. J. Webb, C. Weidenthaler and C. Zlotea, *J. Alloys Compd.*, 2020, **827**, 153548.
18 H. Shang, Y. Zhang, Y. Li, Y. Qi, S. Guo and D. Zhao, *Renewable Energy*, 2019, **135**, 1481–1498.
19 H.-J. Lin, Y.-S. Lu, L.-T. Zhang, H.-Z. Liu, K. Edalati and Á. Révész, *Rare Met.*, 2022, **41**, 1797–1817.
20 L. Zhao, F. Xu, C. Zhang, Z. Wang, H. Ju, X. Gao, X. Zhang, L. Sun and Z. Liu, *Prog. Nat. Sci.: Mater. Int.*, 2021, **31**, 165–179.
21 L. Li, Y. Huang, C. An and Y. Wang, *Sci. China Mater.*, 2019, **62**, 1597–1625.
22 C. Milanese, S. Garroni, F. Gennari, A. Marini, T. Klassen, M. Dornheim and C. Pistidda, *Metals*, 2018, **8**, 567.
23 J. Huot, D. B. Ravnsbaek, J. Zhang, F. Cuevas, M. Latroche and T. R. Jensen, *Prog. Mater. Sci.*, 2013, **58**, 30–75.
24 W. Zhang, X. Zhang, Z. Huang, H.-W. Li, M. Gao, H. Pan and Y. Liu, *Adv. Energy Sustain. Res.*, 2021, **2**, 2100073.
25 Y. Lv and Y. Wu, *Prog. Nat. Sci.: Mater. Int.*, 2021, **31**, 809–820.
26 T. He, H. J. Cao and P. Chen, *Adv. Mater.*, 2019, **31**, 1902757.
27 H. Luo, Y. Yang, L. Lu, G. Li, X. Wang, X. Huang, X. Tao, C. Huang, Z. Lan, W. Zhou, J. Guo and H. Liu, *Appl. Surf. Sci.*, 2023, **610**, 155581.
28 P. Chen, Z. T. Xiong, J. Z. Luo, J. Y. Lin and K. L. Tan, *Nature*, 2002, **420**, 302–304.
29 B. Liu, B. Zhang, J. Yuan, W. Lv and Y. Wu, *Int. J. Hydrogen Energy*, 2021, **46**, 18423–18432.
30 J. Wang, T. Liu, G. Wu, W. Li, Y. Liu, C. M. Araújo, R. H. Scheicher, A. Blomqvist, R. Ahuja, Z. Xiong, P. Yang, M. Gao, H. Pan and P. Chen, *Angew. Chem., Int. Ed.*, 2009, **48**, 5828–5832.
31 H. Cao, Y. Zhang, J. Wang, Z. Xiong, G. Wu and P. Chen, *Prog. Nat. Sci.: Mater. Int.*, 2012, **22**, 550–560.
32 M.-J. Valero-Pedraza, D. Cot, E. Petit, K.-F. Aguey-Zinsou, J. G. Alauzun and U. B. Demirci, *ACS Appl. Nano Mater.*, 2019, **2**, 1129–1138.
33 Y. M. Luo, L. X. Sun, F. Xu and Z. W. Liu, *J. Mater. Chem. A*, 2018, **6**, 7293–7309.
34 J. Yang, R. P. Beaumont, D. T. Humphries, M. C. Jensen and X. Li, *Energies*, 2015, **8**, 9107–9116.
35 J. W. Makepeace, T. He, C. Weidenthaler, T. R. Jensen, F. Chang, T. Vegge, P. Ngene, Y. Kojima, P. E. de Jongh, P. Chen and W. I. F. David, *Int. J. Hydrogen Energy*, 2019, **44**, 7746–7767.
36 Y. Shang, C. Pistidda, G. Gizer, T. Klassen and M. Dornheim, *J. Magnesium Alloys*, 2021, **9**, 1837–1860.
37 Q. Li, Y. Lu, Q. Luo, X. Yang, Y. Yang, J. Tan, Z. Dong, J. Dang, J. Li, Y. Chen, B. Jiang, S. Sun and F. Pan, *J. Magnesium Alloys*, 2021, **9**, 1922–1941.
38 Q. Luo, J. Li, B. Li, B. Liu, H. Shao and Q. Li, *J. Magnesium Alloys*, 2019, **7**, 58–71.
39 J. A. Bolarin, R. Zou, Z. Li, Z. Zhang and H. Cao, *Appl. Mater. Today*, 2022, 101570.
40 K. Wang, X. Zhang, Y. Liu, Z. Ren, X. Zhang, J. Hu, M. Gao and H. Pan, *Chem. Eng. J.*, 2021, **406**, 126831.
41 T.-Z. Si, X.-Y. Zhang, J.-J. Feng, X.-L. Ding and Y.-T. Li, *Rare Met.*, 2021, **40**, 995–1002.
42 Z.-Y. Lu, H.-J. Yu, X. Lu, M.-C. Song, F.-Y. Wu, J.-G. Zheng, Z.-F. Yuan and L.-T. Zhang, *Rare Met.*, 2021, **40**, 3195–3204.
43 X.-S. Liu, H.-Z. Liu, N. Qiu, Y.-B. Zhang, G.-Y. Zhao, L. Xu, Z.-Q. Lan and J. Guo, *Rare Met.*, 2021, **40**, 1003–1007.
44 W. Jiang, H. Wang and M. Zhu, *Rare Met.*, 2021, **40**, 3337–3356.
45 M. Yu, Z. Zhu, H.-P. Li and Q.-L. Yan, *Chem. Eng. J.*, 2021, **421**, 129753.
46 H. Liu, L. Zhang, H. Ma, C. Lu, H. Luo, X. Wang, X. Huang, Z. Lan and J. Guo, *J. Energy Chem.*, 2021, **52**, 428–440.
47 X. L. Zhang, Y. F. Liu, X. Zhang, J. J. Hu, M. X. Gao and H. G. Pan, *Mater. Today Nano*, 2020, **9**, 100064.
48 H. Liu, S. He, G. Li, Y. Wang, L. Xu, P. Sheng, X. Wang, T. Jiang, C. Huang, Z. Lan, W. Zhou and J. Guo, *ACS Appl. Mater. Interfaces*, 2022, **14**, 42102–42112.
49 S. He, G. Li, Y. Wang, L. Liu, Z. Lu, L. Xu, P. Sheng, X. Wang, H. Chen, C. Huang, Z. Lan, W. Zhou, J. Guo and H. Liu, *Int. J. Hydrogen Energy*, 2022, DOI: **10.1016/j.ijhydene.2022.1010.1198**.
50 A. C. Dillon, K. M. Jones, T. A. Bekkedahl, C. H. Kiang, D. S. Bethune and M. J. Heben, *Nature*, 1997, **386**, 377–379.
51 C. Liu, Y. Y. Fan, M. Liu, H. T. Cong, H. M. Cheng and M. S. Dresselhaus, *Science*, 1999, **286**, 1127–1129.
52 R. H. Baughman, A. A. Zakhidov and W. A. de Heer, *Science*, 2002, **297**, 787–792.
53 N. L. Rosi, J. Eckert, M. Eddaoudi, D. T. Vodak, J. Kim, M. O'Keeffe and O. M. Yaghi, *Science*, 2003, **300**, 1127–1129.
54 T. Gamo, Y. Moriwaki, N. Yanagihara, T. Yamashita and T. Iwaki, *Int. J. Hydrogen Energy*, 1985, **10**, 39–47.
55 J. Liang and G. Rao, *Chin. Sci. Bull.*, 1986, **31**, 1861–1863.
56 S. Semboshi, N. Masahashi and S. Hanada, *J. Alloys Compd.*, 2003, **352**, 210–217.
57 **http://www.factsage.com/**.
58 *Smithells Metals Reference Book*, ed. W. F. Gale and T. C. Totemeier, Butterworth-Heinemann, Oxford, 8th edn, 2004, pp. 11-11–11-534.
59 Y. Moriwaki, T. Gamo and T. Iwaki, *J. Less-Common Met.*, 1991, **172–174**, 1028–1035.
60 J. L. Bobet, B. Chevalier and B. Darriet, *Intermetallics*, 2000, **8**, 359–363.
61 H. J. Chuang and S. L. I. Chan, *J. Power Sources*, 1999, **77**, 159–163.

62 P. Zhou, Z. Cao, X. Xiao, L. Zhan, S. Li, Z. Li, L. Jiang and L. Chen, *J. Alloys Compd.*, 2021, **875**, 160035.
63 T. Gamo, Y. Moriwaki, N. Yanagihara and T. Iwaki, *J. Less-Common Met.*, 1983, **89**, 495–504.
64 B.-H. Liu, D.-M. Kim, K.-Y. Lee and J.-Y. Lee, *J. Alloys Compd.*, 1996, **240**, 214–218.
65 X. Guo and E. Wu, *J. Alloys Compd.*, 2008, **455**, 191–196.
66 L. Pickering, M. V. Lototskyy, M. Wafeeq Davids, C. Sita and V. Linkov, *Mater. Today: Proc.*, 2018, **5**, 10470–10478.
67 P. Ma, W. Li and E. Wu, *Int. J. Hydrogen Energy*, 2021, **46**, 34389–34398.
68 W. Li, E. Wu, P. Ma, K. Sun and D. Chen, *Int. J. Energy Res.*, 2013, **37**, 686–697.
69 M. T. Hagström, J. P. Vanhanen and P. D. Lund, *J. Alloys Compd.*, 1998, **269**, 288–293.
70 Y.-H. Xu, C.-P. Chen, W.-X. Geng and Q.-D. Wang, *Int. J. Hydrogen Energy*, 2001, **26**, 593–596.
71 M. Au, F. Pourarian, S. G. Sankar, W. E. Wallace and L. Zhang, *Mater. Sci. Eng., B*, 1995, **33**, 53–57.
72 H. J. Chuang and S. L. I. Chan, *J. Alloys Compd.*, 2001, **314**, 224–231.
73 J. L. Bobet and B. Darriet, *Int. J. Hydrogen Energy*, 2000, **25**, 767–772.
74 Y. Komazaki, M. Uchida, S. Suda, A. Suzuki, S. Ono and N. Nishimiya, *J. Less-Common Met.*, 1983, **89**, 269–274.
75 C. Hong, Y. Zhang and D. Han, *Z. Phys. Chem.*, 1994, **183**, 169–174.
76 M. T. Hagström, S. N. Klyamkin and P. D. Lund, *J. Alloys Compd.*, 1999, **293–295**, 67–73.
77 M. Au, F. Pourarian, S. Simizu, S. Sankar and L. Zhang, *J. Alloys Compd.*, 1995, **223**, 1–5.
78 L. Chen, C. Zheng, F. Zheng, X. Wang and C. Chen, *Rare Met. Mater. Eng.*, 2006, **35**, 1268–1271.
79 H. Guo, S. Zhang, Z. Xu, S. Zhang, C. Lu and L. Shi, *Chin. J. Rare Met.*, 2000, **24**, 224–226.
80 J.-G. Park, H.-Y. Jang, S.-C. Han, P. S. Lee and J.-Y. Lee, *Mater. Sci. Eng., A*, 2002, **329–331**, 351–355.
81 T. Huang, Z. Wu, T. Huang, J. Ni, X. Yu, X. Yu and N. Xu, *Chin. J. of Nonferrous Met.*, 2003, **13**, 91–95.
82 J. Qian, J. Chen and Y. Ye, *Acta Metall. Sin.*, 1987, **23**, 534–536.
83 L. Jiang, Y. Chen, Z. Huang, F. Zhan and H. Tu, *Chin. J. Rare Met.*, 2003, 221–224.
84 H.-L. Chu, Y. Zhang, L.-X. Sun, S.-J. Qiu, F. Xu and H.-T. Yuan, *Int. J. Hydrogen Energy*, 2007, **32**, 1898–1904.
85 F. Block and H.-J. Bahs, *J. Less-Common Met.*, 1984, **104**, 223–230.
86 Y. Morita, T. Gamo and S. Kuranaka, *J. Alloys Compd.*, 1997, **253**, 29–33.
87 S. Li, S. Wang, P. Sheng, Z. Li, Y. Wu and X. Guo, *Chin. J. Rare Met.*, 2019, **43**, 754–764.
88 M. Kazemipour, H. Salimijazi, A. Saidi, A. Saatchi and A. Aref arjmand, *Int. J. Hydrogen Energy*, 2014, **39**, 12784–12788.
89 Z. Peng, Q. Li, J. Sun, K. Chen, W. Jiang, H. Wang, J. Liu, L. Ouyang and M. Zhu, *J. Alloys Compd.*, 2022, **891**, 161791.
90 B. Tu, H. Wang, Y. Wang, R. Li, L. Ouyang and R. Tang, *Int. J. Hydrogen Energy*, 2022, **47**, 14952–14960.
91 S. Nayebossadri and D. Book, *Renewable Energy*, 2019, **143**, 1010–1021.
92 X. Wang, R. Chen, S. Li, L. Chen, H. Ge, G. Fang and C. Chen, *Rare Met. Mater. Eng.*, 2007, **36**, 2216–2219.
93 J. Ye, Z. Li, X. Guo, B. Yuan, L. Jiang, X. Liu, S. Wang, H. Yuan, X. Zhao and J. Ji, *China Pat.*, CN103883874, 2012.
94 M. V. Lototskyy, V. A. Yartys, B. G. Pollet and R. C. Bowman, *Int. J. Hydrogen Energy*, 2014, **39**, 5818–5851.
95 M. V. Lototskyy, V. A. Yartys, B. P. Tarasov, M. W. Davids, R. V. Denys and S. Tai, *Int. J. Hydrogen Energy*, 2021, **46**, 2330–2338.
96 S. N. Klyamkin, V. N. Verbetsky and V. A. Demidov, *J. Alloys Compd.*, 1994, **205**, L1–L2.
97 A. R. Galvis E, F. Leardini, J. R. Ares, F. Cuevas and J. F. Fernandez, *Int. J. Hydrogen Energy*, 2018, **43**, 6666–6676.
98 X. Guo, S. Wang, X. Liu, Z. Li, F. Lü, J. Mi, L. Hao and L. Jiang, *Rare Met.*, 2011, **30**, 227–231.
99 M. Shibuya, J. Nakamura and E. Akiba, *J. Alloys Compd.*, 2008, **466**, 558–562.
100 H. Liu, L. Xu, Y. Han, X. Chen, P. Sheng, S. Wang, X. Huang, X. Wang, C. Lu, H. Luo, S. He, Z. Lan and J. Guo, *Green Energy Environ.*, 2021, **6**, 528–537.
101 A. Kumar, S. Banerjee and S. R. Bharadwaj, *J. Alloys Compd.*, 2015, **649**, 801–808.
102 Q. Zhao, J. Xue, Z. Du and J. Li, *Met. Funct. Mater.*, 2005, **12**, 5–8.
103 M. S. El-Eskandarany, F. Al-Ajmi, M. Banyan and A. Al-Duweesh, *Int. J. Hydrogen Energy*, 2019, **44**, 26428–26443.
104 Y. Hu, H. Zhang, A. Wang, B. Ding and Z. Hu, *Acta Metall. Sin.*, 2003, **39**, 1094–1098.
105 Y. Q. Hu, H. F. Zhang, A. M. Wang, B. Z. Ding and Z. Q. Hu, *J. Alloys Compd.*, 2003, **354**, 296–302.
106 J. H. Dai, X. W. Jiang and Y. Song, *Surf. Sci.*, 2016, **653**, 22–26.
107 V. Khodaparast and M. Rajabi, *Procedia Mater. Sci.*, 2015, **11**, 611–615.
108 M.-Q. Fan, L.-X. Sun and X. Fen, *Trans. Nonferrous Met. Soc. China*, 2010, **20**, 1447–1451.
109 S. Orimo, M. Tabata, H. Fujii, K. Yamamoto, S. Tanioka, T. Ogasawara and Y. Tsushio, *J. Alloys Compd.*, 1994, **203**, 61–65.